Compressive Properties of Additively Manufactured Materials Compared to Foams Traditionally Used for Blunt Force Trauma Protection

J. D. Rossiter[1], A. A. Johnson[1] and G. A. Bingham[1]
[1]Design School, Loughborough University, Loughborough, UK
J.D.Rossiter@lboro.ac.uk, A.Johnson@lboro.ac.uk, G.A.Bingham@lboro.ac.uk

ABSTRACT
The aim of this study is to test currently available additive manufacturing (AM) materials against those used in personal protective clothing (PPC) in sport for blunt force trauma (BFT) protection in sport. Compression was identified as the primary mode of deflection during BFT therefore compression testing was chosen. Compressive stiffness and energy of AM polymers & rubber like materials were compared to those of traditional foam materials. This data will be used demonstrate the difference in behaviour between these materials and those used in AM during compression. Polymer and rubber like materials from three different AM processes were compared to three different foam materials in three different densities. Rubberlike materials absorbed the most energy while polymer samples absorbed very little. Some foam materials absorbed quantities of energy comparable to those absorbed by the rubber-like materials, however, they did so over a greater strain range.

KEYWORDS: Additive Manufacturing; Blunt Force Trauma; Protective Clothing; Compression Testing; Foam

1 INTRODUCTION

Personal protective clothing (PPC) in a sporting context is often used for protection from blunt force trauma (BFT) . Foams are currently the most common material used to provide this protection [1], however, issues such: poor thermal regulation [2], [3]; poor fit [4] and restrictions in movement [5], [6] demonstrate there is still room for improvement with these garments.

Foams are used for BFT protection as they offer exceptional energy absorption under low peak stress. This is due to its cellular structure which produces a three region response to compressive stress. [7]

1. The linear elastic region occurs in the first 5% strain and is characterised by cell wall bending. Only a small amount of energy is absorbed here.
2. The plateau region is characterised by cell wall collapse which causes the structures stiffness to drop. In this region, a large degree of strain occurs with very little change in stress applied. Most of the energy is absorbed here.
3. The densification phase is characterised by the base material compressing and occurs when the top wall of the cell makes contact with the bottom. The structures stiffness rises dramatically and permanent deformation occurs. [7]

Additive manufacturing (AM) is defined as

> "process of joining materi- als to make parts from 3D model data, usually layer upon layer, as opposed to subtractive manufacturing and formative manufacturing methodologies"[8]

This technology can produce highly detailed parts with a level of deign freedom previously unavailable through traditional manufacturing [9]. Research by Craddock 2010 has demonstrated that it is possible to produce cellular structures through AM for the purpose of BFT protection [10]. Johnson et al 2015 also examined the use of AM for stab resistant PPC but without a cellular structure [11]. Inclusion of a cellular structure could potentially improve the performance of this PPC however, in order to design a cellular structure that provides adequate protection, it's important to understand how both cellular structures and the new structures base material act under BFT.

2 METHODS

2.1 Material Specimens

AM Materials

Materials from three different AM processes were tested. Two materials, one polymer and one rubber-like material were tested from each process. The materials and their respective processes are listed below in Table 1:

Table 1-AM Materials

Process	Polymer	Rubber-like
Laser Sintering	PA2200	TPU 92A-1
Extrusion	PLA	Ninjaflex (TPE)
Material Jetting	VeroClear	Tango (rubber-like)

Sample Size

Two sample sizes are used, as shown within Figure 1.

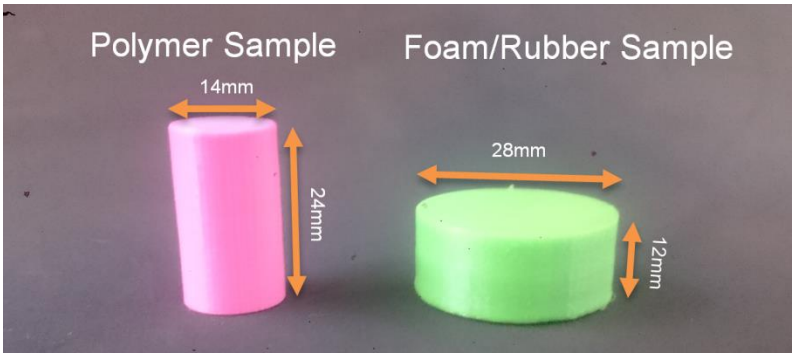

Figure 1-Sample shape and size for polymer samples (left) and rubber-like/foam samples (right)

The polymer sample size used is based on ASTM D695-15 Standard Test Method for Compressive Properties of Rigid Plastic [12]. Foam and rubber samples were shorter with a larger cross sectional area and were established in accordance to ASTM D575-12 Standard Test Methods for Rubber Properties in Compression [13]. Using two different sample sizes allowed all materials to be tested on the same 10kN load cell while still generating useful results.

Foams

Three foam materials were selected based on their prevalence in PPE currently used in sport. These are:

1. Ethylene-Vinyl Acetate (EVA)
2. Polyethylene (PE)
3. XRD Extreme Impact Protection, a impact absorbing foam manufactured by Poron® Urethanes or Rogers Corporation

All foams were tested with three different density samples, one low, one medium & one high.

2.2 Equipment

All compression tests were performed using an Instron 3366 Dual Column Universal Testing System installed with a 10kN load cell (model number: 2530-449) as shown in Figure 2.

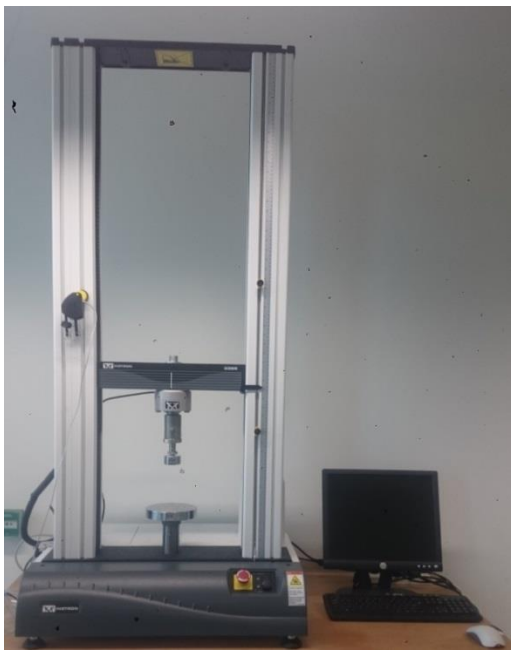

Figure 2-Instron 3366 universal tester

Data was captured via Intron's Bluehill 3 software package.

2.3 Data Collection.

The following steps were taken to record compression data for each material sample:

1. Set the universal tester hard extension limits. Slowly lower the cross heads to the point where the gap between the plates is barely visible. Move the trigger slider up the rail so that it is in contact with the cross heads.
2. Set the strain rate at 1.0/s for loading phase.
3. Set the trigger for unloading phase at 9.5kN. This prevents the load cell internal safety limits being triggered prior to unloading.
4. Set the strain rate at -1.0/s for loading phase.
5. Adjust the top plate position so that it is just above the samples without touching it and set this as the return point.
6. Zero the load cell and start the compression sequence manually.
7. Test five specimens of each material as stipulated by ASTM D695-15.
8. Export data as .csv file

2.4 Data Processing

The following steps were used to process data. All data was imported to and processed through Matlab:

1. Plot graph of the stress strain response.
2. Split loading and unloading response
3. Calculate stiffness for each material using the loading response:
    a. For foams, stiffness calculated separately for each of the three regions: linear elastic, plateau and densification.
    b. For polymers and rubberlike materials where the expected loading response is linear, the stiffness is calculated from the slope of this line.
4. Calculate energy absorbed by sample from area enclosed by hysteresis. This is achieved by subtracting the area of the unloading response from the area of the loading response.
5. Results were reported as the mean of the five specimens of each material

3 RESULTS

Results from compression testing for the rubber-like samples are displayed in Table 1.

Table 2-AM rubber-like material test results: Note that E=refers to young's modulus; W_d=energy absorbed by the foam and ε_{max}=maximum strain exerted on the foam. Stiffness values are in MPa, W_d is recorded In MJ.

	E	W_d	ε_{max}
TPU	35.7146	1.353	0.417
TPE	20.674	1.615	0.602
Tango+	N/A	N/A	N/A

Energy absorption was highest for TPE with TPU in second. Energy Absorbed by TPU was comparable to the level of energy absorbed by PE_HD which was the most absorbent of the foam materials tested.

During testing, the Tango+ samples bulged significantly to the point where cylinder walls of the sample contact the compression plates increasing the cross sectional area. This is displayed in Figure 3.

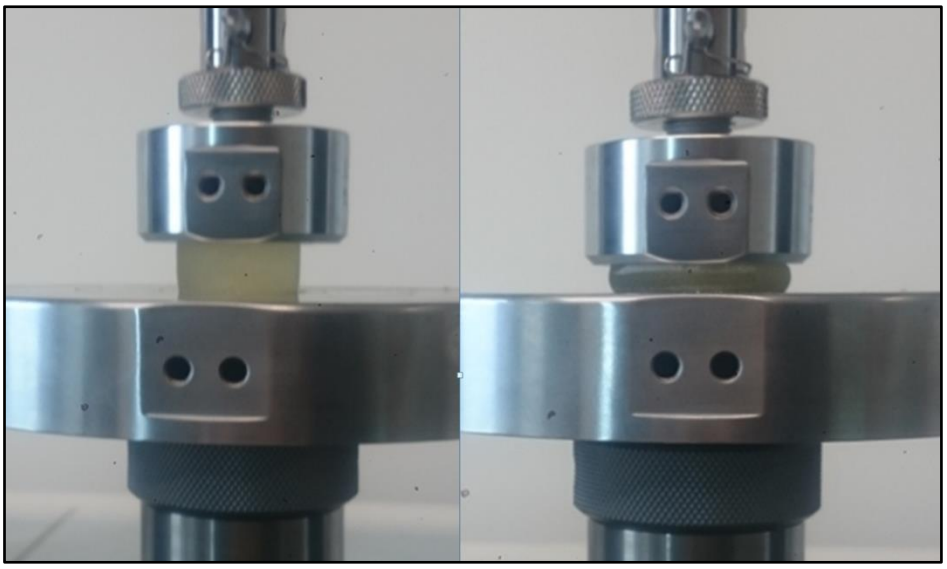

Figure 3-Tango+ bulging under compression

The resulting loading response was curved versus the other two samples in this group which were both linear.

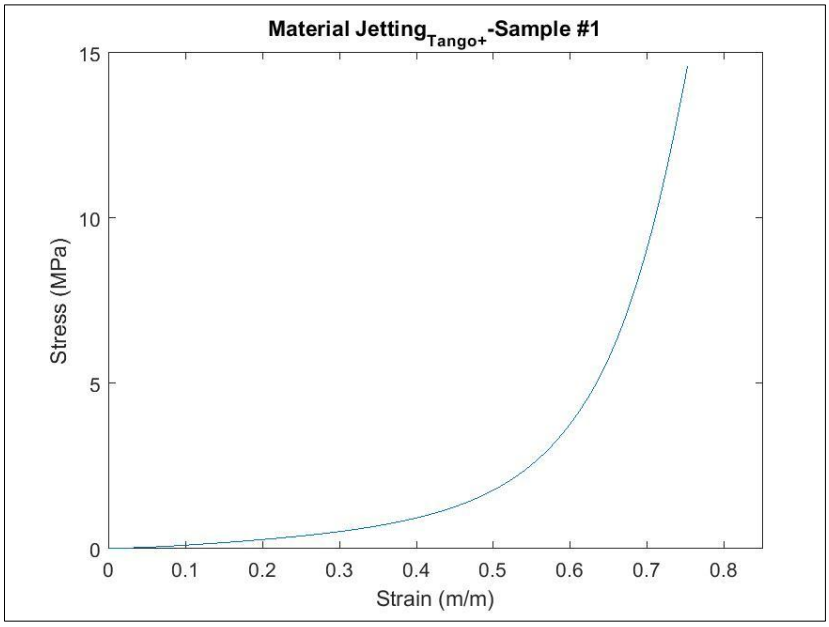

Figure 4-Tango+ loading response

This is likely due to the artificial increase in stress caused by the increasing cross sectional area. Consequently, these results have been excluded.

Results from compression testing for the polymer samples are displayed in Table 3.

Table 3-AM polymer test results: Note that E=refers to young's modulus; W_d=energy absorbed by the foam and ε_{max}=maximum strain exerted on the foam. Stiffness values are in MPa, W_d is recorded In MJ.

E	W_d	ε_{max}

PA2200	988.689	0.651	0.075
PLA	1617.022	0.083	0.044
VeroClear	1731.815	0.051	0.036

Veroclear produced the stiffest samples followed by PLA. PA2200 exceeded its yield strength during testing resulting in a small level of plastic deformation. This also caused in increase in energy absorption compared to the other samples tested.

Results from compression testing for the foam samples are displayed in Table 1.

Table 4-Foam test results: Note that E=refers to compressive modulus where subscript denotes the realavent region of the response; W_d=energy absorbed by the foam and ε_{max}=maximum strain exerted on the foam. Stiffness values are reported in MPa, W_d is reported In MJ.

	E_{Lin}	E_{Plat}	E_{Dens}	W_d	ε_{max}
EVA_HD	12.967	0.787	266.074	1.063	0.823
EVA_MD	10.574	0.803	282.389	0.899	0.810
EVA_LD	3.679	0.289	362.295	0.411	0.937
PE_HD	14.805	0.101	224.458	1.383	0.949
PE_MD	1.840	0.148	432.738	0.239	0.982
PE_LD	N/A	N/A	N/A	N/A	N/A
XRD_HD	0.755	0.181	204.499	0.481	0.858
XRD_MD	0.428	0.067	267.431	0.368	0.902
XRD_LD	0.219	0.030	425.061	0.156	0.902

PE_{LD} was not stiff enough to reach the 9.5kN limit and had to be excluded from testing. Results from the AM polymer materials are displayed in Table 3. While EVA_HD did have a stiffer linear region and absorbed more energy, EVA_MD was stiffer over all undergoing the least maximum strain of all the foams tested. Stiffness of the linear region for all XRD foams was noticeably lower than all other foams.

4 DISCUSSION

Stiffness across the linear elastic region and the plateau region for all foams increased with density, however, stiffness of the densification region was shown to decrease with density. It is worth noting that the densification stiffness tends towards the young's modulus of the foams base material as the foam undergoes further strain. As the lower density foams were more compliant in earlier regions, particularly the plateau, this caused them to reach a higher level of ε_{max} (excluding EVA_{MD} which was 1.3% strain lower than EVA_{HD}). In theory, densification stiffness of foams of the same base material should be very similar in magnitude.

Energy absorption in foams was also shown to increase with foam density. This was expected as higher density foams have a higher ratio of base material to gas. This means that there is a higher contribution of cell wall deformation to the loading response which corresponds to a higher contribution of energy absorbed by the base material though plastic deformation which is the main mechanism of energy absorption in foams [7]. It is interesting to note that the XRD

foam which is marketed as an impact absorbing material showed poor energy absorption compared to the other foams tested.

Energy absorption was highest in the rubber-like AM material group and foams specifically EVA_{HD}, PE_{HD}. However, the way in which this energy is absorbed is quite different as depicted in Figure 5.

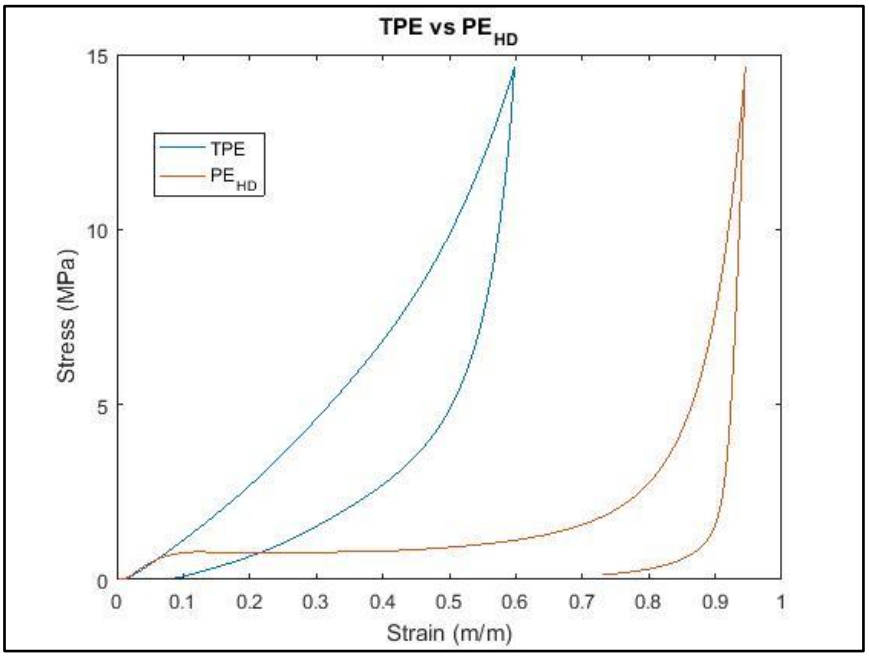

Figure 5-Comparison of energy absorption in TPE and PE_{HD}

These materials have comparable levels of energy absorption for the same peak stress but PE_{HD} absorbs this energy at a much lower rate with a more gradual change in this rate as the foam enters densification. This means that there is a lower impulse experienced by the compression plate in the early stages of compression. Most of the energy is also absorbed at a relatively low stress level during the plateau phase, meaning that for lower energy impacts, peak stress would be considerably lower than those seen in the rubber like materials.

The AM polymers showed very high stiffness values compared to the other examined materials groups. They also displayed very low levels of energy absorption as expected. The resulting level of strain experienced by the material was also comparably low.

Given the success that cellular structures have shown in their ability to absorb energy, it is suggested that the next stage of research utilises AMs design freedom to design so cellular or lattice structures capable of absorbing comparable levels of energy. It is suggested that foam materials, be re-examined at a higher strain rate or under impact to better represent the loading rates experienced by PPC during BFT.

5 CONCLUSION

Based on the findings from this initial investigate, foam materials absorb more energy than the solid AM polymer samples. While the rubber like samples energy absorption capabilities were comparable to those of the foams tested, the plateau region of the foams response allows more energy to be absorbed at a lower stress level. This plateau can only occur due to the collapse

of the foams cellular structure. With this in mind, the next logical step is to explore producing cellular structures using AM.

6 REFERENCES

[1] N. J. MILLS, “Foam protection in sport,” in *Materials in sports equipment*, M. Jenkins, Ed. Boca Raton: Woolshed Publishing Ltd, 2000, pp. 9–44.

[2] G. Havenith, “Heat Balance When Wearing Protective Clothing,” *Br. Occup. Hyg. Soc.*, vol. 43, no. 5, pp. 289–296, 1999.

[3] S. F. Godek *et al.*, “Core Temperature and Percentage of Dehydration in Professional Football Linemen and Backs During Preseason Practices,” *J. Strenght Cond. Res.*, vol. 41, no. 1, pp. 8–17, 2006.

[4] J. Webster, “The perception of comfort and t of personal protective equipment in sport,” Loughborough University, 2010.

[5] P. C. Dempsey, P. J. Handcock, and N. J. Rehrer, “Impact of police body armour and equipment on mobility,” *Appl. Ergon.*, vol. 44, no. 6, pp. 957–961, 2013.

[6] J. Huck, “Protective clothing systems: A technique for evaluating restriction,” *Appl. Ergon.*, no. September, pp. 185–190, 1988.

[7] L. J. Gibson and M. F. Ashby, *Cellular Solids*, 2nd ed. Cambridge: Cambridge University Press, 1997.

[8] ISO and ASTM, “Standard Terminology for Additive Manufacturing – General Principles –,” ISO/ASTM 52900:2015(E), 2015.

[9] I. Gibson, D. W. D. W. Rosen, and B. Stucker, *Additive Manufacturing Technologies: Rapid Prototyping to Direct Digital Manufacturing*, vol. 54. 2009.

[10] J. Brennan-Craddock, “The investigation of a method to generate conformal lattice structures for additive manufacturing,” Loughborough University, 2011.

[11] A. A. Johnson, G. A. Bingham, and C. E. Majewski, “Laser sintered body armour: establishing guidelines for dual-layered stab protection,” *Int. J. Rapid Manuf.*, vol. 5, no. 1, p. 3, 2015.

[12] ASTM, “Standard Test Method for Compressive Properties of Rigid Plastic.pdf,” D695−15, 2015.

[13] ASTM, “Standard Test Methods for Rubber Properties in Compression 1,” D575-12, 2001.